

1993-06

# Cortical Dynamics of Feature Binding and Reset: Control of Visual Persistence

---

<https://hdl.handle.net/2144/2106>

*"Downloaded from OpenBU. Boston University's institutional repository."*

**CORTICAL DYNAMICS OF FEATURE BINDING AND RESET:  
CONTROL OF VISUAL PERSISTENCE**

Gregory Francis, Stephen Grossberg, and Ennio Mingolla

**July, 1992**

**Revised: June, 1993**

**Technical Report CAS/CNS-92-026**

*Vision Research, in press.*

Permission to copy without fee all or part of this material is granted provided that: 1. the copies are not made or distributed for direct commercial advantage, 2. the report title, author, document number, and release date appear, and notice is given that copying is by permission of the BOSTON UNIVERSITY CENTER FOR ADAPTIVE SYSTEMS AND DEPARTMENT OF COGNITIVE AND NEURAL SYSTEMS. To copy otherwise, or to republish, requires a fee and/or special permission.

Copyright © 1992

Boston University Center for Adaptive Systems and  
Department of Cognitive and Neural Systems  
111 Cummington Street  
Boston, MA 02215

# Cortical Dynamics of Feature Binding and Reset: Control of Visual Persistence

Gregory Francis<sup>1</sup>, Stephen Grossberg<sup>2</sup>, and Ennio Mingolla<sup>3</sup>

Center for Adaptive Systems  
and  
Department of Cognitive and Neural Systems  
Boston University  
111 Cummington St.  
Boston, MA 02115<sup>4</sup>  
July, 1992  
Revised: June 1993

Address reprint requests to: Stephen Grossberg.

Running head: Cortical dynamics of binding and reset

**Key Words:** vision, neural networks, visual cortex, visual persistence, feature binding, illusory contours, off-cells.

---

<sup>1</sup>This material is based upon work supported under a National Science Foundation Graduate Fellowship, the Air Force Office of Scientific Research (AFOSR 90-0175) and the Office of Naval Research (ONR N00014-91-J-4100).

<sup>2</sup>Partially supported by the Air Force Office of Scientific Research (AFOSR 90-0175), the Defense Research Projects Agency (AFOSR 90-0083), and the Office of Naval Research (ONR N00014-91-J-4100).

<sup>3</sup>Partially supported by the Air Force Office of Scientific Research (AFOSR 90-0175).

<sup>4</sup>Acknowledgements: Thanks to Diana J. Meyers for her valuable assistance in the preparation of the manuscript.

## Abstract

An analysis of the reset of visual cortical circuits responsible for the binding or segmentation of visual features into coherent visual forms yields a model that explains properties of visual persistence. The reset mechanisms prevent massive smearing of visual percepts in response to rapidly moving images. The model simulates relationships among psychophysical data showing inverse relations of persistence to flash luminance and duration, greater persistence of illusory contours than real contours, a U-shaped temporal function for persistence of illusory contours, a reduction of persistence due to adaptation with a stimulus of like orientation, an increase of persistence due to adaptation with a stimulus of perpendicular orientation, and an increase of persistence with spatial separation of a masking stimulus. The model suggests that a combination of habituating, opponent, and endstopping mechanisms prevent smearing and limit persistence. Earlier work with the model has analyzed data about boundary formation, texture segregation, shape-from-shading, and figure-ground separation. Thus, several types of data support each model mechanism and new predictions are made.

## Introduction

Humans and other animals form useful visual representations of rapidly changing scenes. The visual system rapidly resets the segmentations of changing parts of a scene to prevent image smearing. This article explains how a neural network theory of early visual processes proposed by Grossberg & Mingolla (1985a,b, 1987) accounts for many of the data on visual persistence. The theory suggests that a key process governing these data is the time taken to reset a segmentation. We simulate reset dynamics that help to force a rapid return of the network to a state unbiased by prior segmentation in order to better process incoming data. We explain how hysteresis in the segmentation network is a rate-limiting factor in visual persistence, and show that properties of the hysteresis match key psychophysical data. Psychophysical studies of visual persistence have revealed four key sets of data, which are all explainable by the model:

- Persistence is inversely related to stimulus duration and to stimulus luminance.
- Illusory contours persist much longer than real contours and illusory contours do not obey the inverse relationship between persistence and stimulus duration characteristic of luminance-based contours.
- When subjects adapt to a stimulus of the same orientation as the test stimulus, persistence of the test stimulus decreases; but when subjects adapt to a stimulus of a perpendicular orientation to the test stimulus, persistence of the test stimulus increases.
- The subsequent onset of a masking stimulus greatly curtails persistence of a target stimulus.

Before presenting the details of model mechanisms, we briefly describe how the model addresses each of these data sets.

*Inverse relation of persistence to luminance and to stimulus duration:* Figure 1a, taken from Bowen, Pola, & Matin (1974), shows that, for each luminance curve, persistence is inversely related to stimulus duration. Except for very short stimulus durations, persistence is also inversely related to stimulus luminance. Similar results have been found by many authors (see Coltheart, 1980; Breitmeyer, 1984 for reviews).

In the study of Bowen *et al.* (1974), subjects were asked to match the perceived offset of a target stimulus with the perceived onset of a probe stimulus. The physical interstimulus interval between the target and mask stimuli provided a measure of the target's persistence. Long & Gildea (1981) argued that perceived offset is not a good measure of persistence because some parts of the stimulus may continue to persist beyond the perceived stimulus offset. Sakitt & Long (1979) and Long & McCarthy (1982) showed that when subjects were told to attend to any residual trace of the stimulus, and not just perceived offset, the duration of *total persistence* was directly related to stimulus luminance. Measures of total persistence have, in turn, been criticized as being the result of afterimages or iconic memory (Coltheart, 1980; Breitmeyer, 1984; DiLollo, 1984). Perceived offset and total persistence are thus different features of the dynamic processing of a changing stimulus. In this paper we model persistence data based upon perceived offset, and we do not consider the properties

of total persistence until the conclusion. When we refer to persistence we mean the time between physical offset and perceived offset.

The inverse relationships between persistence and stimulus duration and luminance imply that persistence cannot be modeled as a simple decay of activity of some neural stimulus representation. The initial strength of such a representation at the moment of stimulus offset would presumably increase with stimulus duration or luminance, yielding a higher starting point from which decay would begin, and thus longer persistence. Figure 1b (solid lines) demonstrates that persistence of signals in the model is inversely related to stimulus duration and luminance at all but the shortest durations. The model achieves this close match with the psychophysical data by generating an active reset signal at stimulus offset which inhibits the persisting signals of the stimulus (Grossberg, 1991). We later quantitatively analyze how the strength of the reset signal increases with stimulus duration and luminance.

- Figure 1 -

*Paradoxical increase of persistence of illusory contours:* Figure 2a (taken from Meyer & Ming, 1988) shows that illusory contours have different persistence properties than contours defined by luminance edges. Not only do illusory contours persist substantially longer than real contours, but persistence of an illusory contour peaks at an intermediate stimulus duration. In contrast, the persistence of a stimulus defined by luminance edges continually decreases as stimulus duration increases. These data place strong constraints on the source of signals used to reset a changing visual segmentation. In our model, only changes in luminance-derived edges generate reset signals. Thus, figural boundaries that include illusory contours persist longer than contours of corresponding length that are defined entirely by luminance edges, because the former contain luminance edges as a smaller proportion of the total contour. Figure 2b shows that the model's responses to illusory contours persist longer than real contours. Persistence of illusory contours in the model is not inversely related to stimulus duration at short durations because illusory contours take some time to fully develop (Reynolds, 1981) and, if not fully developed, they can more quickly disappear.

- Figure 2 -

*Effects of orientation-specific adaptation:* Figure 3 (dark bars) shows that adaptation to stimuli can also influence persistence duration (Meyer, Lawson, & Cohen, 1975). This figure demonstrates that when subjects adapted to a stimulus of the same orientation as the test stimulus, persistence of the test stimulus decreased; but when subjects adapted to a stimulus of a perpendicular orientation to the test stimulus, persistence of the test stimulus increased. In each case, persistence could be changed by as much as  $\pm 20$  milliseconds. These data provide two clues about the hypothesized reset signal. First, it suggests that adaptation or habituation drives the reset signal. Second, it indicates that opponent interactions between pathways sensitive to opposite orientations regulate the inhibition that forms the reset signal. Below we explain how a neural circuit consistent with these observations can generate a transient response at stimulus offset that acts as a reset signal. Figure 3 (light bars) shows that adaptation influences persistence of signals in the model in the same way revealed by psychophysical studies.

- Figure 3 -

*Shortening of persistence by a spatially proximal mask:* Figure 4a from Farrell, Pavel, & Sperling (1990) shows that the influence of a mask on the persistence of a target depends on the spatial distance between the stimuli, with closer masks decreasing the persistence of the target. Other studies (Farrell, 1984; DiLollo & Hogben, 1987) have found similar results. Most researchers interpret this result as being due to spatial inhibition, which prevents smearing of moving stimuli. The model contains this type of inhibition and Figure 4b (solid line) demonstrates that the persistence of signals in the model correlates well with the psychophysical data.

The model that we use to simulate persistence data was originally developed to explain many other types of psychophysical and neural data, such as data about boundary completion, illusory contour formation, texture segregation, shape-from-shading, 3-D figure-ground pop-out, brightness perception, and filling-in of 3-D surface percepts (Grossberg, 1987a, 1987b, 1993; Grossberg & Mingolla, 1985a, 1985b, 1987; Grossberg & Todorović, 1988). Model mechanisms have also been derived from several basic principles about visual information processing (Grossberg, Mingolla, & Todorović, 1989). The model's success in simulating persistence data lends greater weight to the physical reality of these mechanisms. Put another way, the fact that the model can explain persistence data without a change of mechanism illustrates its predictive power while linking persistence data to other types of perceptual data that have been explained by the same mechanisms. Grossberg (1993) and Grossberg & Mingolla (1993) summarize a number of experiments that have successfully tested model mechanisms since they were first proposed.

- Figure 4 -

The model proposes two sources of inhibition that reset visual segmentations of stimuli. Upon stimulus offset, interactions of habituation and opponent processing across units tuned to perpendicular orientations generate a reset signal. Spatial inhibition among units of like orientational tuning provides the other inhibitory signal. Other researchers have suggested using a reset signal to control persistence (Breitmeyer, 1984; Ögmen, 1993), but they did not recognize the importance of habituation and opponent processing, or the relation of these properties to the generation and reset of illusory contours. DiLollo & Hogben (1987) and Farrell *et al.* (1990) recognized the role of spatial inhibition in accounting for the data described in Figure 4a, but they did not implement the inhibition in a specific architecture capable of explaining the properties of visual persistence.

Simulations of the model generated Figures 1b, 2b, 3, and 4b with a *single set of parameters* (except where the model is intentionally "dissected" for analysis). All the equations and parameters governing the model behavior are described in the Appendix. These simulations demonstrate the model's competence to explain qualitative relationships between persistence and various stimulus qualities. The simulations do not in every case provide a quantitative match with the psychophysical data. Why this is so is discussed in the concluding remarks.

### Feature Binding as a Source of Visual Persistence

In this section we describe how the Boundary Contour System (BCS) (Grossberg & Mingolla, 1985a,b, 1987) addresses the psychophysical properties of visual persistence. Figure 5 schematizes the model, with each cell's icon drawn to indicate its receptive field structure.

- Figure 5 -

We base our first observation on the adaptation studies of Meyer *et al.* (1975), which show that persistence can be specifically modified according to stimulus orientation. These data are explained using model cells that locate and represent oriented boundaries. Thus, although cells in the first level contain unoriented center-surround receptive fields, the remaining cells in the network respond best to a boundary of a specific orientation. In agreement with neurophysiological data on receptive field properties in visual cortex (Hubel & Wiesel, 1965), the first level of oriented cells in the BCS correspond to cortical simple cells. These cells respond to oriented luminance edges of a specific polarity centered at a particular point on the retina. Cells in the next level, corresponding to complex cells in visual cortex, receive rectified inputs from like-oriented simple cells of each polarity. Model complex cells thus respond to an oriented luminance edge of either polarity.

The orientation-specific habituation identified by Meyer *et al.* (1975) is modeled by a habituating transmitter gate (Grossberg, 1972) placed between each complex cell and its corresponding cell in the next higher level. Figure 5 codes this habituating transmitter gate as a rectangle between the pathways connecting the levels. Whenever a signal passes through this gate, the supply of transmitter is inactivated in proportion to the strength of the signal. Upon offset of the signal, the dynamics of the transmitter gate act to restore the transmitter to its resting level. The dynamic changes in the gates occur at a slower time scale than the activities of neurons, so that a transmitter gate may remain habituated for some time beyond stimulus offset.

Embedded along these pathways is one component of the spatial inhibition implied in Figure 4a. This inhibition occurs from complex cells to the next level of hypercomplex cells. It occurs among hypercomplex cells that are sensitive to edges of the same orientation and nearby spatial positions, and the strength of inhibition falls off with distance. Grossberg & Mingolla (1985a,b) call this process the *first competitive stage*. This competition occurs across positions in the direction of preferred orientational tuning (endstopping) as well as across positions lateral to the preferred direction. Activities from the first competitive stage feed into a process of cross-orientation inhibition at each position called the *second competitive stage*, which partially accounts for the opponent processing implied by the results of Meyer *et al.* (1975) in Figure 3.

Signals surviving the competitive stages input to cooperative *bipole cells* that are sensitive to more global properties of the configuration of image contrasts. Figure 5, for example, shows a horizontally tuned bipole cell, which receives excitatory inputs from a horizontal row of horizontally tuned cells and inhibitory inputs from vertically tuned cells at the same locations. This orientation-specific inhibition helps to explain the orientation-specific data of Meyer *et al.* (1975) in Figure 3. Grossberg & Mingolla (1985b) showed that this inhibition provides the network with a property of *spatial impenetrability*, which prevents boundary linkings from forming across intervening boundaries of roughly perpendicular orientation.

Every bipole cell has two independent lobes to its receptive field, and each lobe must receive a sufficient amount of excitatory input from the second competitive stage for the bipole cell to generate a response. A bipole cell triggers a response only if its receptive fields are each stimulated by one or more boundary components. For example, a bipole cell whose receptive field center is at a corner of a boundary cannot generate a response because the contour stimulates only one side of its receptive field. On the other hand, a bipole cell centered between two illusory contour inducers as in, say, a Kanizsa square, will generate a bipole response if the inputs are sufficiently strong. In this fashion, parallel arrays of bipole cells can generate an illusory contour. Von der Heydt, Peterhans, & Baumgartner (1984) have found evidence supporting the existence of bipole cells in area V2 of monkey cortex.

Bipole-to-hypercomplex feedback carries out a *spatial sharpening* process similar to the first competitive stage. Here, each bipole cell feeds back on-center, off-surround signals to hypercomplex cells of the same orientation sensitivity. Spatial sharpening is another part of the model that correlates with the spatial inhibition indicated in Figure 4a.

The positive feedback from the bipole cells to lower level hypercomplex cells provides the rate-limiting source of persistence in the model because the activities generated by the feedback from one bipole cell can excite parallel arrays of other bipole cells, which in turn feed back signals that can excite the original bipole cell, as indicated in Figure 6a. A self-sustaining feedback loop is generated by the cooperative interactions of the pathways marked by heavy lines. Thus, within the model, persistence is due the positive feedback interactions that choose a coherent boundary segmentation from among many possible groupings, and inhibit potential groupings that are weaker. This positive feedback loop causes hysteresis that is controlled by other model mechanisms.

- Figure 6 -

For example, as indicated in Figure 6b, the end of a surface contour does not support these feedback interactions. In this figure the leftmost boundary signal of Figure 6a has been deleted. Without this boundary signal, the left bipole cell does not fire because only one side of its receptive field receives stimulation. Upon stimulus offset, the effect of this organization is that, even without an active reset signal, the boundary signal at the end of a contour passively decays away and exposes a new contour end (as in Figures 6a → b). At this new contour end, the process repeats itself for another bipole cell and so on from the ends of the surface contour inward toward the middle of the contour (as in Figures 6b → c). It is this inward erosion of boundary signals that we correlate with the persisting visual percept beyond stimulus offset. In the simulations described below, we show that, without an active reset signal, this passive erosion is insufficient to model the psychophysical data on persistence.

Figure 7 summarizes a simulation of boundary signal erosion. Figure 7a shows the stimulus presented to the system, a bright square on a dark background. Figures 7b-d show the boundary signal response to the luminance edges of the stimulus at successive points in time beyond stimulus offset. The figures show the slow erosion of boundary signals from the corners of the stimulus to the middles of the contours. Figure 8 shows the strength of the horizontal boundary signals along the lower edge of the square as they vary over time

beyond stimulus offset. The plot also demonstrates the erosion of boundary signals coding this edge.

- Figure 7 -

- Figure 8 -

### Reset Signals and Gated Dipoles

We now describe how the model generates reset signals upon stimulus offset. Figure 9 shows a subset of the cells from Figure 5. Shown are separate pathways sensitive to the same position in visual space but perpendicular orientations. These pathways compete through the second competitive stage, as described above. Feeding this competition are inputs gated by habituating transmitters. In addition to signals from external stimuli, each input pathway receives a tonic source of activity, which establishes a non-zero baseline of activity that energizes the off-response which occurs after the stimulus terminates. All output signals are rectified. This combination of rectification, opponent competition, habituating transmitter gates, and tonic input produces what Grossberg (1972) called a *gated dipole* circuit. At the offset of stimulation, a gated dipole circuit generates a transient rebound of activity in the previously non-stimulated pathway.

- Figure 9 -

The time plot next to each cell or gate describes the dynamics of this circuit. In the case shown, the sharp increase and then decrease of the time plot at the lower right of Figure 9 indicates that an external input stimulates the horizontal pathway. In response to the stronger signal being transmitted to the next level, the amount of transmitter in the gate inactivates during stimulation and then rises back toward the baseline level upon stimulus offset. Notice that the inactivation and reactivation of transmitter occur more slowly than changes in the activities of the neural cells. Each slowly habituating transmitter multiplies, or gates, the more rapidly varying signal in its pathway, thereby yielding net overshoots and undershoots at input onset and offset, respectively. During stimulation, the horizontal channel wins the opponent competition against the vertical channel as indicated in the top right time plot. However, upon offset of the stimulation to the horizontal channel, the input signal returns to the baseline level but the horizontal transmitter gate remains habituated below its baseline value. As a result, shortly after stimulus offset, the gated tonic input in the horizontal channel has a net signal *below the baseline level*. Meanwhile, the vertical pathway maintains the baseline response at all cells and gates before the opponent competition. Thus, when the horizontal channel is below the baseline activity, after stimulus offset, the vertical channel wins the opponent competition and produces a rebound of activity as shown in the top left time plot. As the horizontal transmitter gate recovers from its habituated state, the rebound signal in the vertical channel weakens and finally disappears.

Figure 10 shows how this rebound of activity acts as a reset signal in the full BCS architecture. Figure 10a schematizes how inputs in a horizontal pathway excite a horizontal bipole cell. As describe above, these horizontal bipole cells can generate a hysteresis that

corresponds to persistence. Due to the interactions of the gated dipole circuit, offset of the horizontal input generates a rebound of activity in the vertical pathway, which, as Figure 10b demonstrates, inhibits the horizontal bipole cell. This inhibition greatly speeds up the erosion of boundary signals and decreases persistence. Note that, apart from its crucial role in explaining persistence data, the inhibition of bipole cells by offset signals from perpendicularly oriented pathways of the gated dipole circuit has been shown to play an equally crucial role in preventing unwanted boundary groupings across intervening surfaces (spatial impenetrability).

- Figure 10 -

The inverse relationships between persistence and stimulus duration and luminance, as shown in Figure 1a, follow from the properties of the gated dipole. The longer the stimulus duration, or the stronger (more luminous) the input to a gated dipole, the more habituated becomes the transmitter gates and, thus, the stronger becomes the reset signals. The significance of the strength of the reset signals is evident in Figure 1b, which shows that persistence of signals in the model is inversely related to stimulus duration and luminance, except at very short stimulus durations. At short stimulus durations, there is only a very weak reset signal generated by the gated dipoles. However, because the stimulus presentation is so brief, the BCS does not establish a strong hysteresis in the feedback loop. Indeed, because stimuli of a greater duration or a higher luminance create stronger boundary signals and can more quickly establish strong activities in the feedback loop, at the shortest stimulus durations persistence is directly related to stimulus duration and luminance. Haber & Standing (1970) reported that persistence increases with stimulus duration when the stimuli are briefer than 20 milliseconds. At longer stimulus durations, the gated dipoles begin to generate stronger reset signals, which more quickly remove the persisting boundary signals in the feedback loop. Thus, the inverse relationships between persistence and luminance and duration occur when a strong hysteresis has been established in the BCS and when the gated dipole circuits produce strong reset signals.

To emphasize the role of the gated dipole circuit and its reset signal, we re-ran simulations for two luminance values and several different stimulus durations but modified one parameter so that the transmitter gates did not habituate. The dotted lines in Figure 1b show that without the transmitter habituation, persistence increases, or does not change, with stimulus duration. Similarly, persistence increases with stimulus luminance without the gated dipole circuit; thus, it is the behavior of habituating transmitters in the gated dipole circuit that explains the data of Bowen *et al.* (1974) within the BCS model.

Because the habituating transmitters of the gated dipole circuit are located outside the feedback loop of the BCS, only the offsets of luminance-derived edges generate reset signals. Therefore, only the reset signals generated by illusory contour inducers inhibit the persisting illusory contours. Inducers of illusory contours have few luminance edges and so, at stimulus offset, generate fewer reset signals than boundaries defined entirely by real contours. With fewer reset signals available to break the hysteresis of the feedback loop, illusory boundaries persist longer than real boundaries. We show the results of simulations of these properties in Figure 2b. The luminous-based stimulus for these simulations was an outline square,

while the illusory contour inducers were L-shaped stimuli at the corners of a square. Our choice of inducer forms was limited by computational resources as explained in detail in the Appendix. This choice suffices to illustrate the dynamical properties of contours that are formed at positions without luminance contrast. Other research concerning the BCS has more fully analyzed the relationships between boundary signals and perceived illusory contours through computer simulation (Gove, Grossberg, & Mingolla, 1993) and psychophysical experimentation (Leshner & Mingolla, 1993). Grossberg & Mingolla (1985a) also analyzed why some inducers produced stronger illusory contours than others.

Because luminance edges define only a small part of an illusory contour, the boundary representation takes longer to become strongly established than the boundary representation of the outline square. Therefore, illusory stimuli of short duration do not generate strong hysteresis and can more quickly erode at stimulus offset. Stimuli of an intermediate duration generate strong hysteresis, but do not produce strong reset signals at offset. Thus, these stimuli persist longest. Stimuli of long duration generate a strong hysteresis, but they also generate stronger reset signals, which shorten persistence. Thus, over the same range of stimulus durations that show an inverse relationship with persistence for the outline square, persistence of boundary signals for an illusory contour is not inversely related to stimulus duration at short durations, but peaks at some intermediate value, as shown in Figure 2b. The darker lines in Figure 2b connect simulation data points of the stimulus durations sampled in the psychophysical studies of Meyer & Ming (1988). A comparison of these curves with the data in Figure 2a shows that they are very similar in shape, although the absolute persistence values are different.

Finally, because the opponent processing and habituating pathways are orientation-specific, the model explains the adaptation results of Meyer *et al.* (1975) shown in Figure 3. Within the model, adaptation to, say, a horizontal stimulus habituates the transmitter in horizontal pathways but leaves the vertical pathways unadapted. If one then tests persistence of a horizontal stimulus, the horizontal pathways further habituate transmitter during the test presentation. The stronger than usual habituation of the horizontal pathways means that, at stimulus offset, the reset signals will be stronger than usual and persistence will decrease. On the other hand, if one tests persistence of a vertical stimulus, then both oriented pathways become habituated: the horizontal pathways from the prior adaptation and the vertical pathway from the habituation due to the target presentation. As a result of the opponent competition between these habituated signals (Figure 9), the reset signals generated at offset of the vertical test stimulus will be weaker than usual and persistence will increase.

So far we have accomplished two major goals. First, we explained how interactions of a tonic input, habituating transmitter gates, opponent processing, and rectified output signals in a gated dipole circuit generate a reset signal upon offset of an oriented luminance edge. Second, we showed that the properties of this reset signal at the second competitive and bipole stages of the model account for the inverse relationships between persistence and stimulus luminance and duration (Bowen *et al.*, 1974), the prolonged non-monotonic persistence properties of illusory contours (Meyer & Ming, 1988), and the opposite influences on persistence of orientation-specific adaptation (Meyer *et al.*, 1975).

It remains to show that the spatial inhibition, or endstopping process, within the first

competitive stage of the model can account for the decrease in persistence shown in Figure 4a. The solid line in Figure 4b demonstrates that the persistence of boundary signals does depend on the separation between target and mask stimuli. For comparison, the dashed line shows the persistence of boundary signals when we removed the oriented spatial competition of the first competitive stage from the model (setting one parameter equal to zero). The second source of spatial inhibition, in the feedback pathway of the bipole cells, remains intact. In the current simulations it is of a smaller range than the interactions of the first competitive stage. The dashed line in Figure 4b shows that without the spatial competition there are no changes in persistence of the target stimulus until the target and mask boundaries are within the range of the inhibition in the feedback pathway. Thus, the spatial competition accounts for the ability of the masking stimulus to reduce persistence of the target (Farrell *et al.*, 1990).

### Neurophysiological Correlates and Predictions

Grossberg (1987a) reviews neural analogs of all stages of the present model in visual cortex. In particular, von der Heydt *et al.* (1984) found analogs of bipole cells in area V2 of monkey visual cortex, which Cohen & Grossberg (1984), Grossberg (1984), and Grossberg & Mingolla (1985a) had modelled before these data were published. It may be possible to use additional neurophysiological studies to verify the dynamic properties of these cells. For example, it should be possible to observe the inward erosion of boundary signals by observing a single bipole cell in visual cortex. After finding the center of the bipole cell's receptive field, one could run a series of experiments varying the position of luminance edges relative to the center of the cell's receptive field. Because the model predicts that boundary signals erode from the contour ends, the cell should show its greatest persisting response when its receptive field is centered on the contour and should show less persistence as the experimenter shifts the contour center to one side or the other of the receptive field center. Note that this prediction follows despite another prediction, derived from an analysis of the BCS in response to static stimuli, that before stimulus offset the *amplitude* of activity should be nearly identical for bipole cells all along the contour, regardless of the cell's distance from inducers before reset occurs. Properties such as the inverse relationships between persistence and stimulus duration and luminance, greater persistence for illusory than real contours, the effects of adaptation, and the influence of a masking stimulus should also be observable in an investigation of these cells.

Likewise, the ability of masking stimuli to reduce persistence of the target should be measurable at a suitable population of hypercomplex cells. Other hypercomplex cells should exhibit habituated gating of their responses, as well as opponent rebounds to offset of stimuli that are oriented perpendicular to their receptive fields. The firing of these rebounding hypercomplex cells should correlate with diminished persistence in target bipole cells that are tuned to a perpendicular orientation.

Leshner & Mingolla (1993) have tested the BCS model through psychophysical experiments on the induction of illusory contours in a Kanizsa square using variable numbers of line ends that are perpendicular to the illusory contour. They found that an inverted  $U$  function relates

illusory contour clarity to the number of line end inducers. The BCS explains the inverted  $U$  as follows. More line end inducers at first produce more cell activations at hypercomplex cells of the second competitive stage whose receptive fields are centered at and perpendicular to the line ends. These responses are called *end cuts* (Grossberg & Mingolla, 1985b). They are due to an interaction between the first and second competitive stages. The first competitive stage inhibits those hypercomplex cells at a line end whose orientational preference is parallel to the line. These inhibited cells disinhibit (via the second competitive stage) hypercomplex cells at the line end whose orientational preference is perpendicular to the line (see Figure 5). These greater numbers of end cuts, in turn, colinearly cooperate to more strongly activate the bipole cells that generate the illusory contour.

As more line inducers are used, however, they get closer together. They then inhibit each others' target hypercomplex cells via lateral inhibitory signals from the first competitive stage. Their net responses are hereby weakened by lateral inhibition, as are their end cuts and their illusory contours. Leshner & Mingolla (1993) noted that other models of illusory contour formation cannot explain this inverted  $U$  effect.

The BCS model suggests that an inverted  $U$  function may also relate illusory contour persistence to the number of line end inducers under these experimental conditions, since weaker bipole cell activations should erode more quickly after stimulus offset and since a greater number of reset signals would be generated. That is, as the spatial density of line inducers increases beyond the point where illusory contour clarity reverses, then illusory contour persistence should also reverse in response to line inducers that are on for a fixed amount of time. Stimuli in the rising portion of the Leshner & Mingolla (1993) study provide both stronger bipole cell activity and stronger reset signals, and so present a more ambiguous case. This type of experiment would probe the interactions between first and second competitive stages, as well as between the spatial and temporal properties of emergent segmentation.

Grossberg (1987a, Section 30) linked properties of the BCS simple, complex, and hypercomplex cells to experimentally reported properties of spatial localization and hyperacuity. Badcock & Westheimer (1985a, 1985b) used flanking lines to influence the perceived location of a test line. They varied the position of the flank with respect to the test line as well as the direction-of-contrast of flank and test lines with respect to the background. They found that two separate underlying mechanisms were needed to explain their data: a mechanism concerned with the luminance distribution within a restricted region, and a mechanism reflecting interactions between features. Within the central zone defined by the first mechanism, sensitivity to direction-of-contrast was found, as would be expected within an individual receptive field. On the other hand, a flank within the surround region always caused a repulsion which is independent of direction-of-contrast. Thus "when flanks are close to a target line, it is pulled toward the flank for a positive flank contrast but they push each other apart if the flank has a negative contrast. A flank in the surround region always causes repulsion under the conditions presented" (p. 1263). To further test independence of direction-of-contrast due to the surround, they also found that "the effect of a bright flank on one side can be cancelled by a dark flank on the other. Within the central zone this procedure produces a substantial shift of the mean of a positive contrast target line towards the positive contrast flank" (p. 1266).

Badcock & Westheimer (1985a) noted that the average of luminance within the central zone is sensitive to amount-of-contrast and direction-of-contrast in a way that is consistent with a Difference-of-Gaussian model. Such a computation also occurs at the elongated receptive fields, or input masks, of the BCS (Figure 5). Pairs of simple cells with like positions and orientations but opposite directions-of-contrast then add their rectified outputs at complex cells which are, as a consequence, insensitive to direction-of-contrast (Figure 5). Such cells provide the inputs to the first competitive stage. The oriented short-range lateral inhibition at the first competitive stage is thus insensitive to direction-of-contrast, has a broader spatial range than the central zone, and, being inhibitory, would always cause repulsion – all properties of the Badcock & Westheimer (1985a) data. In summary, all the main effects in these data mirror properties of the circuit in Figure 5.

In further tests of the existence and properties of these distinct mechanisms, Badcock & Westheimer (1985b, p. 3) noted that “in the surround zone the amount of repulsion obtained was not influenced by vertical separation of the flank halves, even when they were several minutes higher (or lower) than the target line. In the central zone attraction was only obtained when the vertical separation was small enough to provide some overlap of lines in the horizontal direction.” These data further support the idea that the central zone consists of individual receptive fields, whereas the surround zone is due to interactions across receptive fields which are first processed to be independent of direction-of-contrast, as in Figure 5. In our computer simulations of boundary completion and segmentation (Grossberg & Mingolla, 1985a, 1985b), it was assumed that the lateral inhibition within the first competitive stage is not restricted to any preferred orientation, as is also true of the surround repulsion effect in the Badcock & Westheimer (1985b) data.

This theoretically predicted correlation between properties of hyperacuity, persistence, and illusory contour formation presents an opportunity to design new types of psychophysical experiments with which to further test the model. Other new experimental opportunities are summarized in Grossberg (1993). Some of these are now being explored in our laboratory.

### **Related Findings and Concluding Remarks**

Because the equations presented in the Appendix are for a “single-scale” BCS, they cannot explain findings by Meyer & Maguire (1981) that the persistence of a grating percept increases with spatial frequency. However, the multiple scale BCS interactions described in Grossberg (1993) can account for this finding without affecting the explanations described in this paper. With multiple scales of oriented filters, a grating of a low spatial frequency excites both large and small filters, whereas a grating of a high spatial frequency excites only small scaled filters. The net result of this skewed excitation distribution across scales is that the low spatial frequency grating creates more reset signals than the high spatial frequency grating. All activated filters of similar orientational and disparity sensitivity at each position input to the same set of bipole cells. As in the case of real versus illusory contours, more reset signals imply less persistence.

The model also suggests why different experimental methods find different properties of persistence (Sakitt & Long, 1979). The results in this paper have correlated the disappearance of boundary signals with the perceived offset of the stimulus. However, due to the

slow time constants of the habituation in the gated dipole circuit, reset signals generated at stimulus offset may persist beyond the offset of the boundary signals. Perceptual awareness of these reset signals may be used by subjects when the experimental instructions tell them to observe any residual trace of the stimulus, as in the studies of Sakitt & Long (1979). In particular, stronger luminance implies greater habituation, which implies a greater length of time for the rebounding channels of the gated dipole to return to baseline. Thus, the persistence of the reset signals may be directly related to stimulus luminance, in agreement with the psychophysical studies of total persistence (Sakitt & Long, 1979; Nisly & Wasserman, 1989).

In reading the Appendix, note that a single set of parameters was used to simulate all the properties of visual persistence. While modifying the parameters may change the quantitative values given in Figures 1, 2, 3, and 4, the relevant functional properties expressed by the curves remain the same. Specifically, regardless of the specific choice of parameters (excluding cases where boundary signals or reset signals are not created at all), persistence of signals in the model is inversely related to stimulus luminance and duration, illusory contours persist longer than real contours, orientation-specific adaptation has opposite influences on persistence, and a spatial masking stimulus inhibits target persistence. The relationships between persistence and stimulus properties are built into the structure, or non-parametric design, of the model. In the present simulations, our goal has thus been to clarify and illustrate the qualitative functional meaning of persistence data. In much the same way, quantitative persistence values vary from subject to subject and with experimental conditions. This being said, it needs also to be noted that no alternative explanation of persistence properties has explained as wide a range of data, provided the level of detail implemented herein, or attributed these properties to fundamental design constraints on the dynamic balance that regulates perceptual resonance and reset.

Given that the entire structure and dynamics of the model had previously been derived and tested on other data than persistence data, the model's ability to simulate the important functional properties of persistence data lends even greater support to the neural reality of these model mechanisms. The ability of this same small set of model mechanisms to explain data from several perceptual and neural paradigms also provides conceptual linkages across paradigms whereby new types of experiments can be designed to further test these mechanisms.

In summary we have shown how an analysis of the BCS cortical model can offer new mechanistic and functional explanations of data on visual persistence. These explanations are consistent with the theory's previous explanations of boundary completion (Grossberg & Mingolla, 1985a), texture segregation (Grossberg & Mingolla, 1985b), shape-from-shading (Grossberg & Mingolla, 1987), and 3-D vision (Grossberg, 1987b, 1993), among others, while extending its explanatory range still further into the difficult temporal phenomena of visual persistence. The functional role of the feature binding and reset mechanisms that the model predicts to be responsible for persistence suggests links between persistence and fundamental issues in the formation and breakup of perceptual groupings in a dynamically fluctuating environment. Thus, far from being esoteric laboratory phenomena, data on persistence afford important clues about some of the most fundamental processes of preattentive vision,

processes moreover that are being increasingly well characterized by neural network architectures.

### Appendix: Network Equations and Parameters

The simulations of the model are a simplification of the system's interactions described elsewhere (Grossberg & Mingolla, 1985a,b, 1987). These simplifications were necessitated by the following fact. Simulations in the prior reports of the model concerned the *spatial* interactions of the segmentation system and so had no need to implement the temporal dynamics of resonance and reset, whose juxtaposition of fast and slow time scales greatly increased the computational load in simulations. To manage this load, the experimental stimuli were also simplified, as indicated in the text without losing their essential characteristics. Thus, the quantitative matches of simulations to data are less significant in this paper than the analysis of how model mechanisms work together to explain the complex qualitative pattern of persistence data. These qualitative properties are, moreover, robust. In much the same way, different psychophysical studies of persistence do not produce identical quantitative values across observers, but do show consistent relationships between persistence and stimulus properties. The psychophysical studies of persistence also do not give absolute measures, but provide only relative values that can be ordered within an experimental paradigm.

The model contains a total of eight levels of model neurons or transmitter gates. Each level, except for the first, consists of two parallel pathways coding horizontal and vertical orientations at each pixel location. Within the second level, each orientation-specific pathway contains two simple cells responsive to opposite polarities of luminance gradients. Thus, associated with each pixel point of the image are seventeen different cells and transmitter gates. Since we carried out all simulations on a  $40 \times 40$  pixel array, the simulated network contained 27,200 cells and transmitter gates. A differential equation describes the behavior of each cell and gate.

We eased the computational requirements of integrating 27,200 differential equations with a number of simplifications. First, rather than integrate all the differential equations explicitly, we algebraically computed some cell activities at the equilibrium value of the differential equation. We made this simplification for the unoriented on-center, off-surround cells in Level 1, the oriented polarity-specific simple cells of Level 2, and the hypercomplex cells undergoing lateral inhibition in Level 4. Computing the values of these cells at equilibrium makes the assumption that they operate on a faster time scale than the other cells. Since the rate-limiting time scales of the simulations involve dynamics of habituating transmitter gates and feedback within the BCS, unfolding the dynamics of these cells would not adversely affect our explanations of visual persistence but would greatly increase the computation required to simulate the model.

A second simplification took advantage of symmetries in the image plane. If the images presented to the system on the left and right sides of the plane are mirror images, then activities produced on the right half will have corresponding equal values on the left. Thus, to save computation, we could compute only the values on the right side of the image plane and extrapolate the results to account for the full image plane. Similarly, when the top and bottom quadrants of the right side are mirror images, we only needed to compute the cell responses on the bottom quadrant. Finally, if the upper and lower diagonals in the quadrant are mirror images, then the values of the horizontal cells in the lower (upper) diagonal equal the values of the vertical cells in the upper (lower) diagonal. Thus, by restricting the

input stimuli to be square-shaped, we only had to integrate the differential equations for the horizontal cells in the bottom right of the image plane to account for the behavior of the entire system.

These simplifications reduced the system of 27,200 differential equations to only 1600 differential equations. The LSODA integrator routine (Petzold & Hindmarsh, 1987) performed the integration of these equations. We based all the network equations upon those described in Grossberg & Mingolla (1985b).

*Level 0: Image Plane.*

Each pixel has a value associated with retinal luminance. We describe the pixel-luminance values of the different stimuli used in the simulations below.

*Level 1: Center-Surround Cells.*

The activity  $X_{ij}^1$  of a Level 1 cell centered at position  $(i, j)$  obeys a shunting on-center, off-surround equation

$$\frac{dX_{ij}^1}{dt} = -X_{ij}^1 + (A - X_{ij}^1) \sum_{pq} B_{ijpq} I_{pq} - (X_{ij}^1 + C) \sum_{pq} D_{ijpq} I_{pq}, \quad (1)$$

where  $I_{pq}$  is the retinal luminance at position  $(p, q)$ ,  $A$  is the maximum activity of the cell,  $-C$  is the minimum activity of the cell, and

$$B_{ijpq} = B \exp[-\alpha^{-2} \log 2[(i-p)^2 + (j-q)^2]] \quad (2)$$

$$D_{ijpq} = D \exp[-\beta^{-2} \log 2[(i-p)^2 + (j-q)^2]] \quad (3)$$

are excitatory and inhibitory Gaussian weighting functions, respectively. The term  $\log 2$  means the parameters  $\alpha$  and  $\beta$  set the radius of their respective Gaussians at half strength. Parameters  $B$  and  $D$  are constant scaling terms.

To save computation, the equilibrium response of the differential equation is found by setting the left hand side of equation (1) equal to zero. The resulting algebraic equation can be solved to find

$$X_{ij}^1 = \frac{A \sum_{pq} B_{ijpq} I_{pq} - C \sum_{pq} D_{ijpq} I_{pq}}{1.0 + \sum_{pq} (B_{ijpq} + D_{ijpq}) I_{pq}}. \quad (4)$$

The activities of cells at this level share some key properties with those found in ganglion cells or LGN (Grossberg, 1987a). No off-center on-surround cells were implemented in our simulations.

*Level 2: Oriented Simple Cells.*

The following equations define oriented simple cells that are centered at position  $(i, j)$  with preferred orientation  $k$ . To create a vertically oriented input field, or in-field, that is specific to the polarity of the luminance gradient, divide an elongated region into a left half  $L_{ijk}$  and a right half  $R_{ijk}$ . Add up the weighted sum of the Level 1 inputs within the range of the left side

$$R_{ijk} = \sum_{pq \in L_{ijk}} E_{ijpq} X_{pq}^1 \quad (5)$$

and the right side

$$G_{ijk} = \sum_{pq \in R_{ijk}} E_{ijpq} X_{pq}^1 \quad (6)$$

of the region, with

$$E_{ijpq} = \exp[-\gamma^{-2} \log 2(i-p)^2] \quad (7)$$

decreasing for inputs further away from the oriented center-line of the in-field the parameter  $\gamma$  controls the rate of fall off. Then a simple cell that is selectively responsive to a bright-to-dark luminance gradient obeys the differential equation

$$\frac{dX_{ijk}^{2BD}}{dt} = -X_{ijk}^{2BD} + [F_{ijk} - G_{ijk}]^+, \quad (8)$$

where  $[p]^+ = \max(p, 0)$ . A cell responsive to a dark-to-bright luminance gradient obeys the equation

$$\frac{dX_{ijk}^{2DB}}{dt} = -X_{ijk}^{2DB} + [G_{ijk} - F_{ijk}]^+. \quad (9)$$

To save computation, the activities of these cells were computed at equilibrium as:

$$X_{ijk}^{2BD} = [F_{ijk} - G_{ijk}]^+, \quad (10)$$

and

$$X_{ijk}^{2DB} = [G_{ijk} - F_{ijk}]^+. \quad (11)$$

### *Level 3: Oriented Complex Cells.*

Each cell in Level 3 becomes insensitive to the polarity of contrast by summing the rectified activities of the cells in Level 2 of the same location and orientation. Each Level 3 cell obeys the differential equation

$$\frac{dX_{ijk}^3}{dt} = -X_{ijk}^3 + H(X_{ijk}^{2BD} + X_{ijk}^{2DB}). \quad (12)$$

Parameter  $H$  scales the activities of the input signals to the complex cell.

### *Level 4: Habituated Transmitter Gates.*

The signal in each oriented pathway is gated, or multiplied, by a habituated transmitter which obeys the following equation (Grossberg, 1972)

$$\frac{dX_{ijk}^4}{dt} = K[L(M - X_{ijk}^4) - (X_{ijk}^3 + J)X_{ijk}^4]. \quad (13)$$

This equation says that the amount of available transmitter  $X_{ijk}^4$  accumulates to the level  $M$ , via term  $KL(M - X_{ijk}^4)$ , and is inactivated by mass action at rate  $K(X_{ijk}^3 + J)X_{ijk}^4$ , where  $J$  is the tonic input of a gated dipole and  $X_{ijk}^3$  is its phasic increment. We always set the rate  $K$  much smaller than 1.0 so that these equations operate on a slower time scale than the equations describing cell activities. At the beginning of each simulation, each transmitter value is set to the non-stimulated equilibrium value  $X_{ijk}^4 = LM/(L + J)$ .

*Level 5: First Competitive Stage of Hypercomplex Cells.*

The gated signals of a fixed orientation compete via on-center off-surround spatial interactions. Along with the tonic signal coming up through the habituating transmitters, each cell also receives a tonic input which supports disinhibitory activations at the next competitive stage (see Grossberg & Mingolla, 1985a,b). The activity of a Level 5 cell obeys differential equation

$$\frac{dX_{ijk}^5}{dt} = -X_{ijk}^5 + J + (X_{ijk}^3 + J)X_{ijk}^4 + NX_{ijk}^8 - X_{ijk}^5 \sum_{pq} P_{ijpq} (X_{pqk}^3 + J)X_{pqk}^4, \quad (14)$$

where  $-X_{ijk}^5$  models the passive decay, the parameter  $J$  establishes a non-zero baseline of activity for the cell, the term  $(X_{ijk}^3 + J)X_{ijk}^4$  is the gated excitatory input from the lower level at the same position and orientation, the term  $NX_{ijk}^8$  is a feedback signal from the higher level cell of the same position and orientation, and the term  $X_{ijk}^5 \sum_{pq} P_{ijpq} (X_{pqk}^3 + J)X_{pqk}^4$  is the inhibitory input from the lower level cells of the same orientation and nearby spatial positions. The inhibitory weights fall off in strength as the spatial distance between cells increases, as in

$$P_{ijpq} = P \exp[-\delta^{-2} \log 2[(i-p)^2 + (j-q)^2]], \quad (15)$$

where  $P$  scales the strength of the inhibition, and  $\delta$  controls the spread.

For the simulations in this paper, the differential equation was solved at equilibrium as

$$X_{ijk}^5 = \frac{J + (X_{ijk}^3 + J)X_{ijk}^4 + NX_{ijk}^8}{1.0 + \sum_{pq} P_{ijpq} (X_{pqk}^3 + J)X_{pqk}^4}. \quad (16)$$

*Level 6: Second Competitive Stage of Hypercomplex Cells.*

The output signals from the first competitive stage compete across orientation at each position. The activity of a cell receiving this competition obeys the differential equation

$$\frac{dX_{ijk}^6}{dt} = -X_{ijk}^6 + (X_{ijk}^5 - X_{ijk}^5) \quad (17)$$

where  $X_{ijk}^5$  and  $X_{ijk}^5$  represent orthogonal orientations.

*Level 7: Cooperative Bipole Cells and Spatial Impenetrability.*

The next level uses a simplified version of bipole cells. As in Level 1, we divide the in-field of each horizontal bipole cell into a left side  $L_{ijk}$  and a right side  $R_{ijk}$  (top and bottom for vertically oriented bipole cells). Each bipole cell then sums up excitatory like-oriented signals and inhibitory orthogonally-oriented signals within each side. A slower-than-linear bounded function squashes the net signal of each side. We then set the output threshold of the bipole cells so that boundaries must stimulate both sides of the receptive field for the cell to generate an output signal. The differential equation describing each bipole cell activity is

$$\frac{dX_{ijk}^7}{dt} = -X_{ijk}^7 + f\left(\sum_{pq \in R_{ijk}} [X_{pqk}^6]^+ - [X_{pqk}^6]^+\right) + f\left(\sum_{pq \in L_{ijk}} [X_{pqk}^6]^+ - [X_{pqk}^6]^+\right) \quad (18)$$

where

$$f(w) = \frac{Qw}{1.0 + w} \quad (19)$$

acts to squash the net input on each side of the bipole cell's receptive field so that it never exceeds the value of parameter  $Q$ . Grossberg & Mingolla (1985b) use a more complicated bipole cell. Their bipole cells receive excitatory inputs from a range of orientations that are weighted by a function that decreases with spatial distance from  $(i, j)$  and orientational difference from  $k$ . Grossberg & Mingolla (1985b) use these features to explain a variety of grouping phenomena, but simpler bipole cells suffice to simulate the basic properties of boundary signal persistence.

#### *Level 8: Spatial Sharpening.*

Output signals from the bipole cells are thresholded to prevent feedback unless inputs activate both sides. These output signals then undergo a spatial sharpening much as in the first competitive stage of Level 5. The activities of cells in Level 8 obey the differential equation

$$\frac{dX_{ijk}^8}{dt} = -X_{ijk}^8 + [X_{ijk}^7 - R]^+ - X_{ijk}^8 \sum_{pq \in S_{ij}} T[X_{pqk}^7 - R]^+ \quad (20)$$

where parameter  $R$  is the output threshold for bipole cells, parameter  $T$  scales the strength of the spatial inhibition, and  $S_{ij}$  is the eight nearest neighbors to pixel  $(i, j)$ . These signals are scaled by parameter  $N$  before feeding back to the cells in Level 5 to close the feedback loop.

#### *Computation of Images and Persistence.*

We operationally defined the boundaries of an image to be persisting whenever, after target offset, a cell in Level 6 at the location and orientation of the target image edge (real or illusory) had an activity value greater than 0.5. The computer checked the values every 0.5 time steps after stimulus offset (one time unit in the simulation is equivalent to ten milliseconds). For all simulated images a value at each pixel in simulated foot Lamberts indicated luminance intensity. The background luminance was always  $10^{-6}$  simulated foot lamberts.

The simulated luminances and durations of the target flashes for Figure 1b are indicated in the figure and were all bright squares ( $26 \times 26$  pixels) on a dark background.

The inducers for the illusory stimuli in Figure 2b were luminance increments (pixel values of 0.15 simulated foot lamberts) in the shape of L's oriented appropriately in each quadrant to line up the inducer edges. The real stimulus was a bright outline (3 pixels wide) square of the same luminance and size ( $32 \times 32$  pixels) as the illusory square.

We did not simulate the remaining stimuli shown in Figure 2a because the simplified BCS used in our simulations creates boundary signals between the inducing stimuli for all of the stimulus sets. It is not the focus of this paper to show that our simulations accurately create illusory contours. Rather, we investigated the persistence of boundaries generated without a luminance edge. Illusory contours are one example of these types of boundary signals. A full simulation of the BCS with more orientations, and whose bipole cell weights are modulated in two dimensions of spatial position and one of orientation, can accurately

predict the generation of illusory contours (Gove *et al.*, 1993). Such a simulation is beyond the scope of this paper.

The test stimulus for Figure 3b was a pair of horizontally oriented luminance bars ( $10 \times 1$  pixels, pixel values of 0.15 simulated foot lamberts) separated by three pixel spaces. The adaptation stimulus was either identical to the test stimulus or six small vertical lines ( $4 \times 1$  pixels each) evenly spaced and placed to intersect with the horizontal bars of the test stimulus. The adaptation and test stimuli were both presented for 100.0 simulated milliseconds.

The target for Figure 4b was a bright square of  $20 \times 20$  pixels with a pixel luminance value of 0.323 simulated foot lamberts. The mask for Figure 4b consisted of a bar ( $16 \times 2$  pixels) along each edge of the target with equal pixel luminance and an edge-to-edge separation from the target of 3 to 9 pixel spaces, each pixel space corresponding to 0.05 degrees of visual angle. Larger spatial separations could not be used due to the limited size of the simulation plane. We always presented the target flash for a duration of 50.0 simulated milliseconds, and matched its offset with the onset of the mask. We kept the masking flash on until the boundaries of the target flash fell below threshold.

#### *Parameter selection.*

Because integration of nonlinear differential equations is computationally expensive, we simplified the BCS equations as much as possible. As a result, we could not use the same parameters as other simulations of the BCS, which calculated the equilibrium response of the system (Cruthirds, *et al.*, 1992; Gove, Grossberg, & Mingolla, 1993; Grossberg & Mingolla, 1985a,b, 1987; Grossberg, Mingolla, & Williamson, 1993). In particular, whereas the present simulations used only vertically and horizontally oriented cells, other BCS simulations have used oblique orientations as well.

To remain consistent with earlier simulations and to explain the properties of persistence, the parameters used in our simulations were required to meet several properties. First, the parameter set had to allow the BCS to locate oriented boundaries. For example, if  $P$  is set too large, then spatial inhibition between cells of like orientation and nearby positions can mutually inhibit activities at the next layer so much that no signal survives the competition. Similarly, the threshold for the bipole cell activities,  $R$ , cannot be set too large (relative to the parameter  $Q$  and the strength of the inputs to the bipole cells) or the bipole cells will never fire.

A second requirement of the parameter set was that the activities in the feedback loop, once activated, needed to be strong enough to persist once the external inputs were turned off. The parameters  $N$ ,  $Q$ ,  $R$ , and  $T$  in the bipole feedback pathway control this property of the network. These parameters were set to insure a persisting activity in the network and proper creation of boundary signals.

Figure 11a shows how the strength of activities in the feedback loop influences persistence. Parameter  $N$  scales the strength of the bipole feedback pathway to the lower stages. Increasing  $N$  strengthens the boundaries in the BCS without changing the strength of the reset signals. Figure 11 shows the persistence of a 100 simulated milliseconds, 0.323 foot lamberts stimulus. Figure 11a shows that as  $N$  increases, persistence also increases because the hysteresis in the feedback loop is stronger.

- Figure 11 -

A third requirement of the parameter set was that it had to allow generation of reset signals upon stimulus offset. This was realized by properly choosing parameters  $J$ ,  $K$ ,  $L$ , and  $M$ , of the habituating transmitter gates. Grossberg (1980, Appendix E) showed that the strength of the reset signal increases with parameter  $M$  and decreases as  $J$  or  $L$  are increased. These parameters also establish the lower limit (equilibrium) of the gate strength. If the gate was allowed to habituate too much, it would no longer pass on sufficient input to the higher levels. In such a case, boundaries could disappear *before* the offset of the stimulus. It is easy to find parameters which avoid this problem. Parameter  $K$  controls the relative rate of habituation, and increasing  $K$  allows for faster habituation and stronger reset signals. Figure 11b shows that increasing  $K$  decreases persistence.

The final task of parameter setting was to control the value of the inputs to the habituating gates so that they created a strong feedback loop and generated strong reset signals. The six parameters of Level 1 act to compress the cell response to luminous inputs. Equation (1) could have been replaced with a function like  $\log(I_{ij})$  to get similar results, but we choose equation (1) to remain consistent with other simulations of the BCS (Gove *et al.*, 1993; Cruthirds *et al.*, 1992). This stage of compression explains why the two lower curves of Figure 1 have similar persistence despite the fact that the stimulus of the lower curve is significantly more luminous. The parameters of Levels 2 and 3 simply scale the activities of the oriented filters. Increasing the activities of these cells has two effects. First, stronger signals create stronger activities in the feedback loop, which act to increase persistence. At the same time, these stronger signals increase habituation to generate stronger reset signals upon stimulus offset. The balance of these factors determines persistence. Figure 11c shows that as parameter  $H$  increases from 0.005 to 0.025 persistence increases. This increase in persistence indicates that the influence of the additional strength given to the activities in the feedback loop is greater than the additional habituation caused by the stronger inputs. As  $H$  increases still further, the additional habituation, and stronger reset signals, tend to dominate the increases in boundary signal strength. This same analysis was used to explain the inverted-U shapes of the curves in Figure 1b and Figure 2b, as a function of stimulus duration.

For our explanations of persistence properties, the only “disallowed” values of parameters are ones that would generate absurd consequences even outside the domain of visual persistence. For example, parameters could be set to prevent bipole cells from performing boundary completion. However, once they are set so as to permit completion, illusory contours persist longer than real contours. That the data curves can be explained through an analysis of the model network *architecture* shows that the persistence properties of the model are robust.

The network parameters remained unchanged across all simulations, only the image luminances, durations, or spatiotemporally adjacent stimuli were varied. The following parameters were used:  $A = 67.5$ ,  $B = 2.5$ ,  $C = 60.0$ ,  $D = 0.05$ ,  $H = 0.1$ ,  $J = 20.0$ ,  $K = 0.0003$ ,  $L = 3.0$ ,  $M = 5.0$ ,  $N = 13.0$ ,  $P = 0.0005$ ,  $Q = 0.5$ ,  $R = 0.61$ ,  $T = 0.3$ ,  $\alpha = 0.5$ ,  $\beta = 3.0$ ,  $\gamma = 1.5$ ,  $\delta = 3.0$ . Each side of the oriented masks in Level 2,  $L_{ijk}$ ,  $R_{ijk}$ , were rectangles of  $4 \times 1$  pixels in size. Each side of a bipole cell was restricted to a single column (vertical)

or row (horizontal) extending 18 pixels from the position of the bipole cell. For comparison purposes, the dashed lines in Figure 1b were computed with  $K = 0.0$ ; and the dashed line in Figure 4b was computed with  $P = 0.0$ .

All simulations were carried out on an Iris 4/280 or an Iris 8/280 Silicon Graphics Superminicomputer. The computation of each simulated data point in Figures 1b, 2b, 3, and 4b, required approximately half an hour on a multi-user machine.

## Bibliography

- Badcock, D.R. & Westheimer, G. (1985a). Spatial location and hyperacuity: The centre/surround localization contribution function has two substrates. *Vision Research*, *25*, 1259-1267.
- Badcock, D.R. & Westheimer, G. (1985b). Spatial location and hyperacuity: Flank position within the centre and surround zones. *Spatial Vision*, *1*, 3-11.
- Bowen, R., Pola, J., & Matin, L. (1974). Visual persistence: Effects of flash luminance, duration and energy. *Vision Research*, *14*, 295-303.
- Breitmeyer, B. (1984). *Visual masking: An integrative approach*. New York: Oxford University Press.
- Cohen, M.A. & Grossberg, S. (1984) Neural dynamics of brightness perception: Features, boundaries, diffusion, and resonance. *Perception & Psychophysics*, *36*, 428-456.
- Coltheart, M. (1980). Iconic memory and visible persistence. *Perception & Psychophysics*, *27*, 183-228.
- Cruthirds, D., Gove, A., Grossberg, S., Mingolla, E., Nowak, N., & Williamson, J. (1992). Processing of synthetic aperture radar images by the boundary contour system and feature contour system. Technical Report CAS/CNS-TR-92-010, Boston, MA: Boston University. *Proceedings of the World Congress on Neural Networks*, Hillsdale, NJ: Lawrence Erlbaum Press, in press.
- DiLollo, V. (1984). On the relationship between stimulus intensity and duration of visible persistence. *Journal of Experimental Psychology: Human Perception and Performance*, *10*, 754-769.
- DiLollo, V. & Hogben, J. (1987). Suppression of visible persistence as a function of spatial separation between inducing stimuli. *Perception & Psychophysics*, *41*, 345-354.
- Farrell, J. (1984). Visible persistence of moving objects. *Journal of Experimental Psychology: Human Perception and Performance*, *10*, 502-511.
- Farrell, J., Pavel, M., & Sperling, G. (1990). The visible persistence of stimuli in stroboscopic motion. *Vision Research*, *30*, 921-936.
- Gove, A., Grossberg, S., & Mingolla, E. (1993). Brightness perception, illusory contours, and corticogeniculate feedback. Technical Report CAS/CNS-TR-93-021, Boston, MA: Boston University. *Proceedings of the World Congress on Neural Networks*, Hillsdale, NJ: Lawrence Erlbaum Press, in press.
- Grossberg, S. (1972). A neural theory of punishment and avoidance: II. Quantitative theory. *Mathematical Biosciences*, *15*, 253-285.
- Grossberg, S. (1980). How does a brain build a cognitive code? *Psychological Review*, *87*, 1-51.
- Grossberg, S. (1984). Outline of a theory of brightness, color, and form perception. In E. Degreef & J. van Buggenhout (Eds.), *Trends in mathematical psychology*. Amsterdam: Elsevier/North-Holland, pp. 59-86.

- Grossberg, S. (1987a). Cortical dynamics of three-dimensional form, color, and brightness perception I: Monocular theory. *Perception & Psychophysics*, *41*, 97-116.
- Grossberg, S. (1987b). Cortical dynamics of three-dimensional form, color, and brightness perception II: Binocular theory. *Perception & Psychophysics*, *41*, 117-158.
- Grossberg, S. (1991). Why do parallel cortical systems exist for the perception of static form and moving form? *Perception & Psychophysics*, *49*, 117-141.
- Grossberg, S. (1993). 3-D vision and figure-ground separation by visual cortex. *Perception & Psychophysics*, in press.
- Grossberg, S. & Mingolla, E. (1985a). Neural dynamics of form perception: Boundary completion, illusory figures, and neon color spreading. *Psychological Review*, *92*, 173-211.
- Grossberg, S. & Mingolla, E. (1985b). Neural dynamics of perceptual grouping: Textures, boundaries, and emergent segmentations. *Perception & Psychophysics*, *38*, 141-171.
- Grossberg, S. & Mingolla, E. (1987). Neural dynamics of surface perception: Boundary webs, illuminants, and shape-from-shading. *Computer Vision, Graphics, & Image Processing*, *37*, 116-165.
- Grossberg, S. & Mingolla, E. (1993). Neural dynamics of motion perception: Direction fields, apertures, and resonant grouping. *Perception & Psychophysics*, *53*, 243-278.
- Grossberg, S., Mingolla, E., & Todorović, D. (1989). A neural network architecture for preattentive vision. *IEEE Transactions on Biomedical Engineering*, *36*, 65-84.
- Grossberg, S., Mingolla, E., & Williamson, J. (1993). Processing of synthetic aperture radar images by a multiscale boundary contour system and feature contour system. Technical Report CAS/CNS-TR-93-024, Boston, MA: Boston University. *Proceedings of the World Congress on Neural Networks*, Hillsdale, NJ: Lawrence Erlbaum Press, in press.
- Grossberg, S. & Todorović, D. (1988). Neural dynamics of 1-D and 2-D brightness perception: A unified model of classical and recent phenomena. *Perception & Psychophysics*, *43*, 241-277.
- Haber, R. & Standing, L. (1970). Direct measures of short-term visual storage. *Quarterly Journal of Experimental Psychology*, *21*, 43-54.
- Hubel, D. & Wiesel, T. (1965). Receptive fields and functional architecture in two nonstriate visual areas (18 and 19) of the cat. *Journal of Neurophysiology*, *27*, 229-289.
- Leshner, G. & Mingolla, E. (1993). The role of edges and line-ends in illusory contour formation. *Vision Research*, In press.
- Long, G. & Gildea, T. (1981). Latency for the perceived offset of brief target gratings. *Vision Research*, *21*, 1395-1399.
- Long, G. & McCarthy, P. (1982). Target energy effects on Type I and Type II visual persistence. *Bulletin of the Psychonomic Society*, *19*, 219-221.
- Meyer, G., Lawson, R., & Cohen, W. (1975). The effects of orientation-specific adaptation on the duration of short-term visual storage. *Vision Research*, *15*, 569-572.

- Meyer, G. & Maguire, C. (1981). Effects of spatial-frequency specific adaptation and target duration on visual persistence. *Journal of Experimental Psychology: Human Perception and Performance*, 7, 151-156.
- Meyer, G. & Ming, C. (1988). The visible persistence of illusory contours. *Canadian Journal of Psychology*, 42, 479-488.
- Nisly, S. & Wasserman, G. (1989). Intensity dependence of perceived duration: Data, theories, and neural integration. *Psychological Bulletin*, 106, 483-496.
- Öğmen, H. (1993). A neural theory of retino-cortical dynamics. *Neural Networks*, 6, 245-273.
- Petzold, L. & Hindmarsh, A. (1987). LSODA: Livermore solver for ordinary differential equations, with automatic method switching for stiff and nonstiff problems.
- Reynolds, R. (1981). Perception of illusory contours as a function of processing time. *Perception*, 10, 107-115.
- Sakitt, B. & Long, G. (1979). Cones determine subjective offset of a stimulus but rods determine total persistence. *Vision Research*, 19 1439-1441.
- von der Heydt, R., Peterhans, E., & Baumgartner, G. (1984). Illusory contours and cortical neuron responses. *Science*, 224, 1260-1262.

### Figure Captions

**Figure 1.** (a) Persistence is inversely related to flash luminance and flash duration. (Reprinted with permission from Bowen *et al.* (1974).) (b) Computer simulation of boundary signal persistence as a function of flash duration and flash luminance. Dashed lines simulate model performance *without* habituative transmitter gates that form the basis of the reset mechanism required to explain data on persistence.

**Figure 2.** (a) Illusory contours persist longer than real contours. Persistence of illusory contours is maximal at an intermediate duration of the stimulus. (Reprinted with permission from Meyer & Ming (1988).) (b) Computer simulation of real and illusory boundary contour persistence as a function of flash duration. The boundaries produced in response to the illusory contours persist longer than the boundaries produced in response to the real contours. Persistence of illusory contours peaks at an intermediate stimulus duration, as in the data. The solid lines connect the points sampled in the data of Meyer & Ming (1988).

**Figure 3.** (Black bars) Change in persistence depending on whether the adaptation stimulus had the same or orthogonal orientation as the test grating. (Plotted from data in Meyer *et al.* (1975).) (Gray bars) Computer simulation of boundary signal persistence depending on whether the adaptation stimulus had the same or orthogonal orientation as the test grating.

**Figure 4.** (a) The persistence of thin lines moving in stroboscopic motion depends on the spatial separation between successive images. (Reprinted with permission from Farrell *et al.* (1990).) (b) Computer simulation of boundary signal persistence as a function of the spatial separation between contours of a target and a mask. Dashed line simulates model performance without the spatial competition. Note that the size of our simulation plane did not permit testing spatial separations larger than shown.

**Figure 5.** Boundary Contour System with embedded gated dipoles. See text for details.

**Figure 6.** (a) Darker lines mark pathways of a closed feedback loop. A bipole cell response can excite an additional bipole cell. The response of that bipole cell can, in turn, excite the original bipole cell. (b) A bipole cell centered above the end of a contour is outside the feedback loop because it receives inputs only on one side of its receptive field. As a result, the boundary signal at that location passively decays away at stimulus offset. (c) After the boundary signal at this location decays away, it exposes a new contour end, and another bipole cell drops out of the feedback loop.

**Figure 7.** (a) Stimulus input to the system, a bright square on a dark background. (b) Boundary response to the square shortly after the input returns to the background level. (c) Boundary signals start to erode from the corners of the square toward the middle of the contours. (d) Boundary erosion is almost complete.

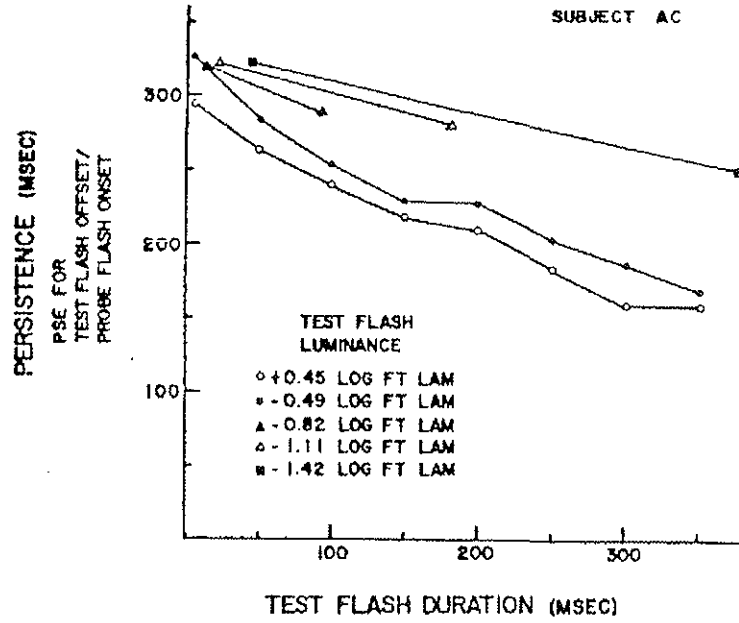
**Figure 8.** Time plot of boundary signal activities at a cross-section of Figure 7 (lower horizontal contour). The signals drop markedly upon stimulus offset as the bottom-up input is removed. The top-down signals maintain the boundaries for a substantial length of time, but the boundaries erode away from the ends toward the middle of the contour.

**Figure 9.** At stimulus offset, a gated dipole circuit produces a transient rebound of activity in the non-stimulated opponent pathway.

**Figure 10.** (a) A horizontal input excites a horizontal bipole cell, which supports persistence. (b) Upon offset of the horizontal input, a rebound of activity in the vertical pathway inhibits the horizontal bipole cell. This inhibition resets the hysteresis of the feedback loop and reduces persistence.

**Figure 11.** Changes in persistence as parameters are modified. In each case only one parameter is varied. The large filled dots mark persistence with the default parameter value. (a) Parameter  $N$  in equation (14) scales the strength of the bipole pathway feedback signals. Increasing parameter  $N$  strengthens the feedback signals to generate a stronger hysteresis in the network without affecting the strength of the reset signals. Persistence increases with  $N$ . (b) Parameter  $K$  in equation (13) controls the rate of habituation of the transmitter gates. Greater habituation makes stronger reset signals, so persistence decreases as  $K$  increases. (c) Parameter  $H$  scales the inputs to the habituating gates in equation (12). Increasing  $H$  creates a stronger resonance and stronger reset signals. Starting with small values, increasing  $H$  has a larger effect on the hysteresis than on the strength of the reset signals, thus persistence increases. At larger values, increasing  $H$  has a larger effect on the strength of the reset signals than on the hysteresis, thus persistence decreases.

(a)



(b)

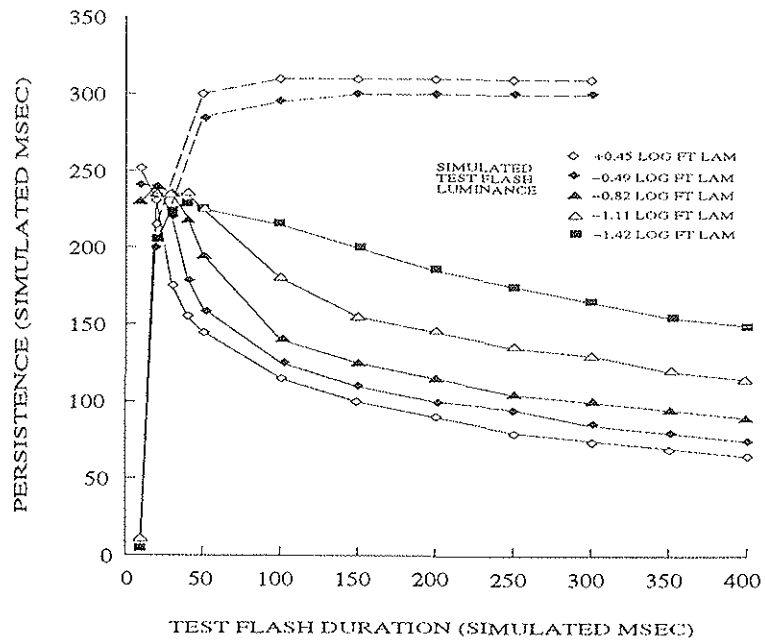
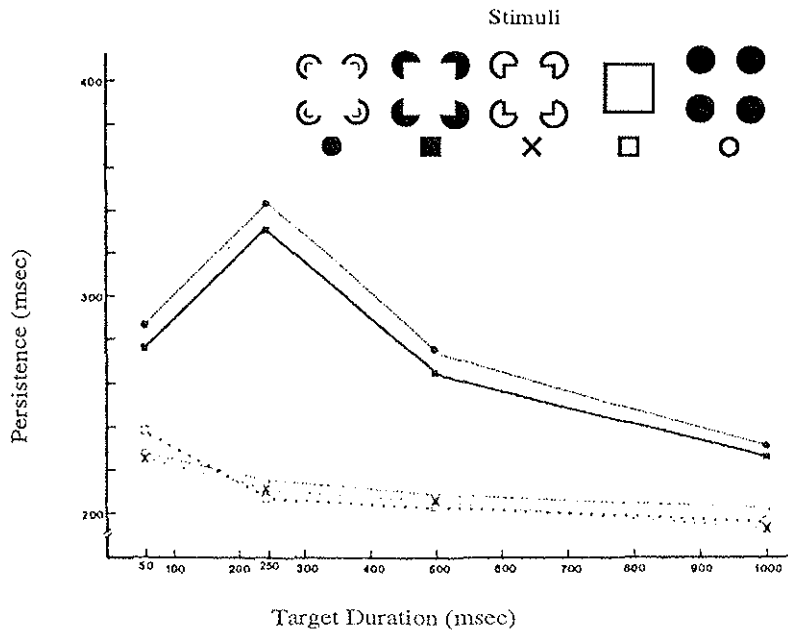


Figure 1:

(a)



(b)

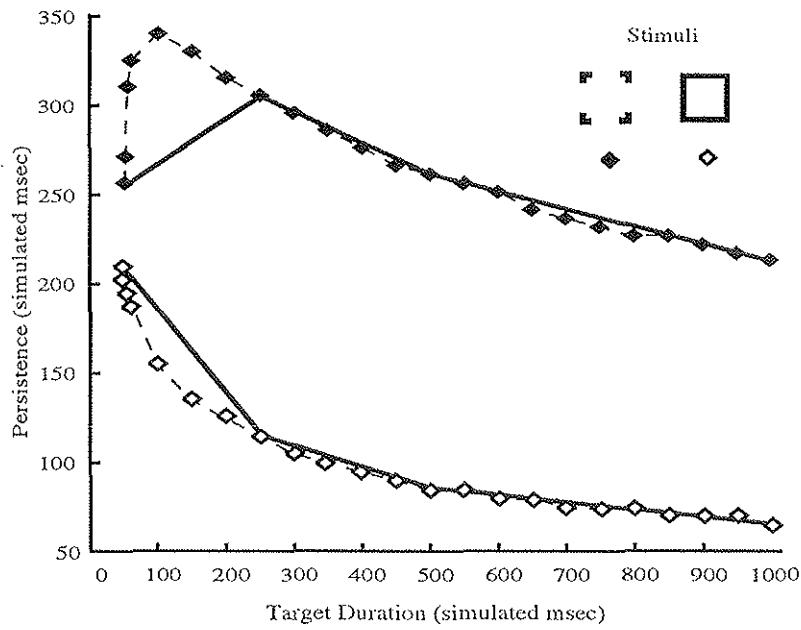


Figure 2:

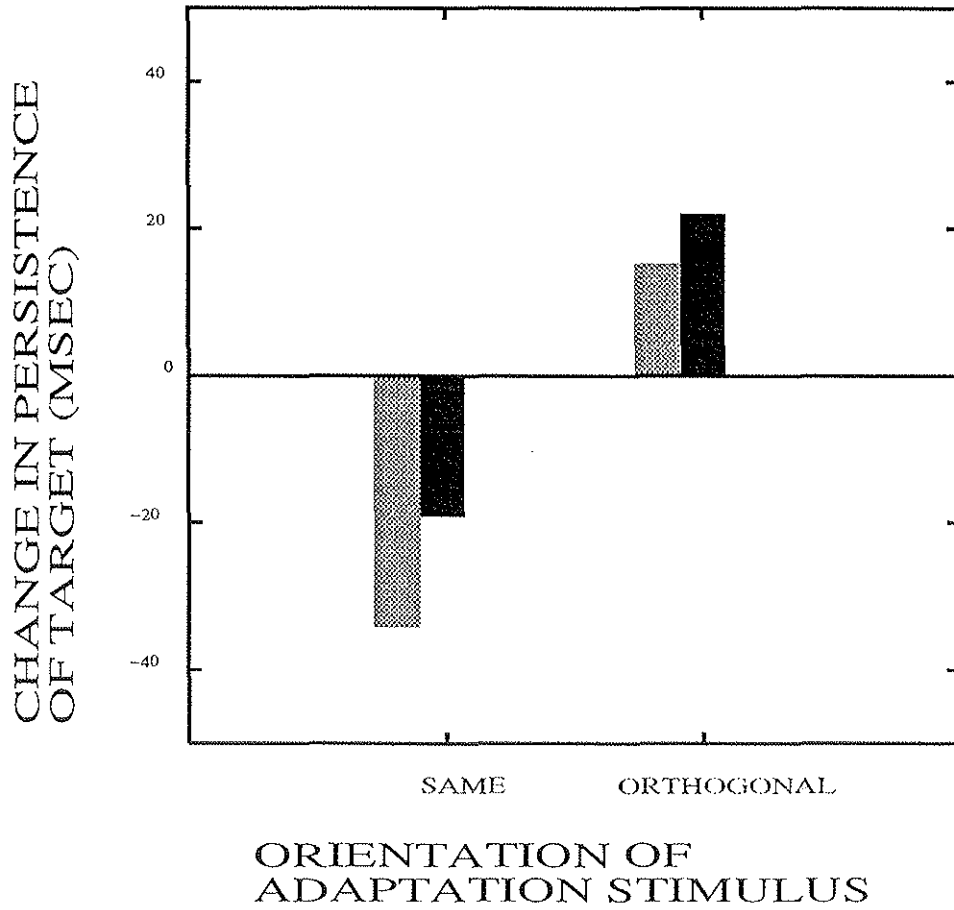
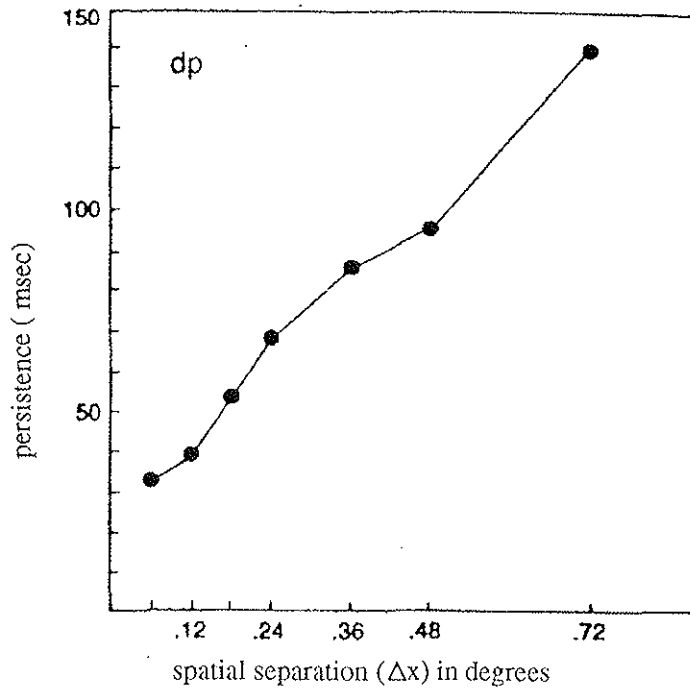


Figure 3:

(a)



(b)

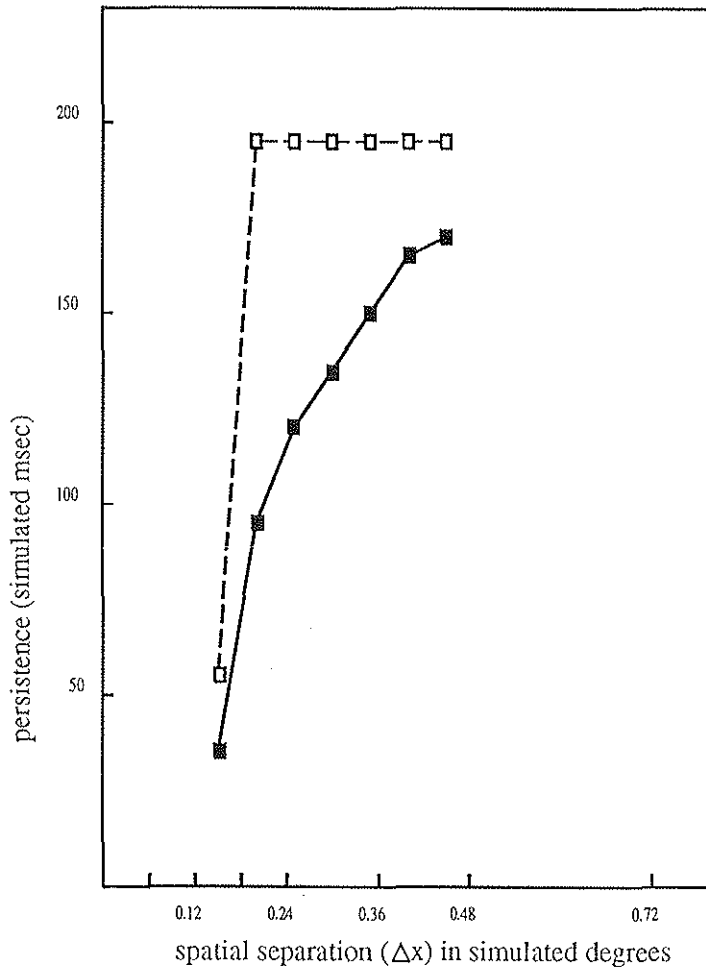


Figure 4:

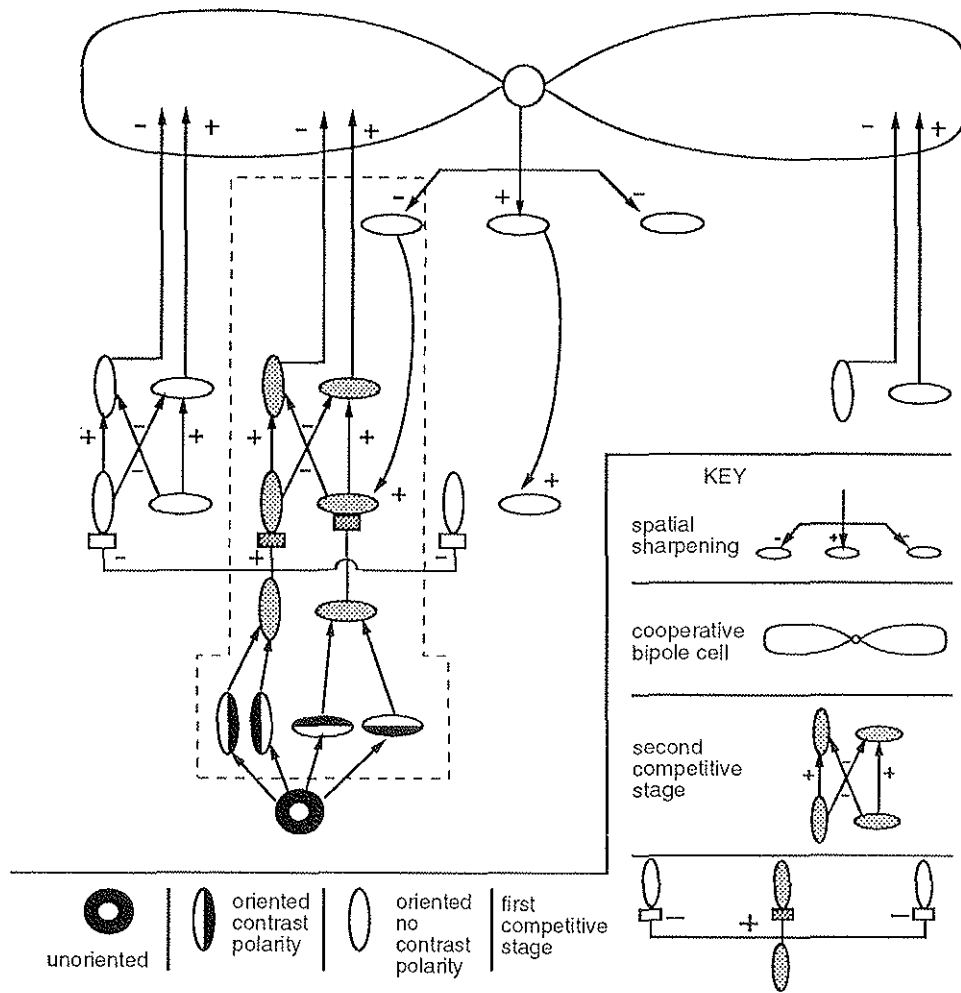
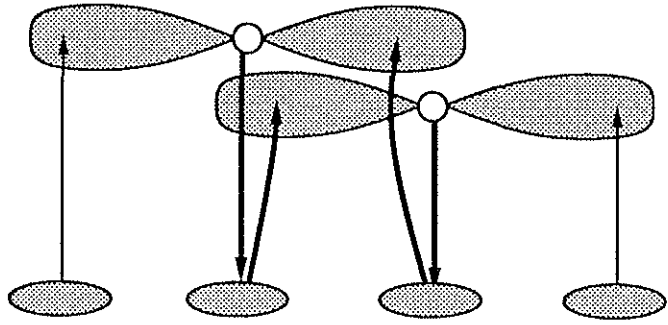
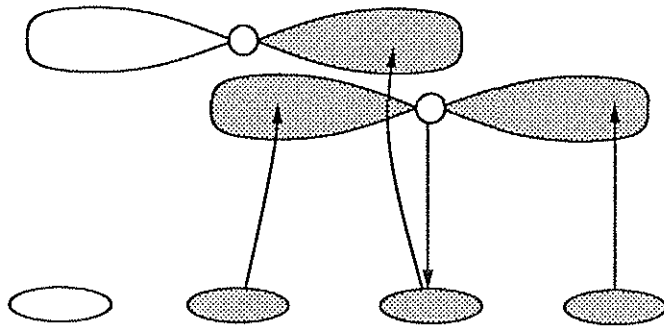


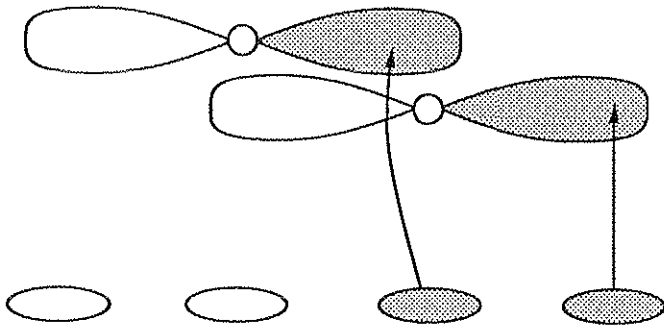
Figure 5:



(a)

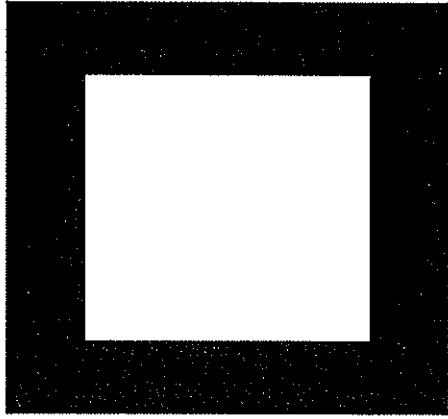


(b)

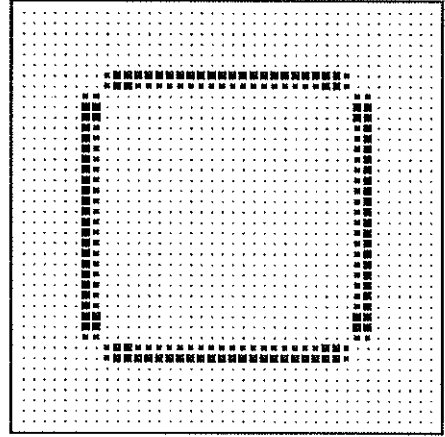


(c)

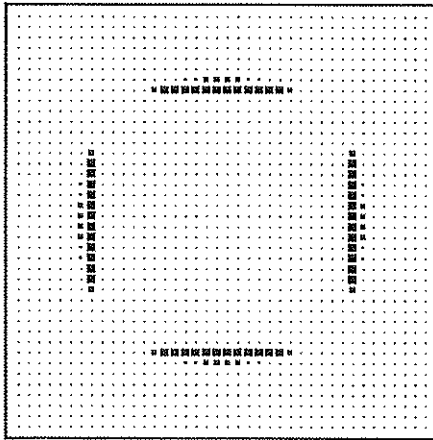
Figure 6:



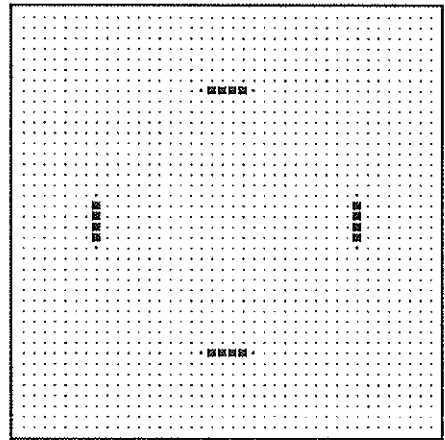
(a)



(b)



(c)



(d)

Figure 7:

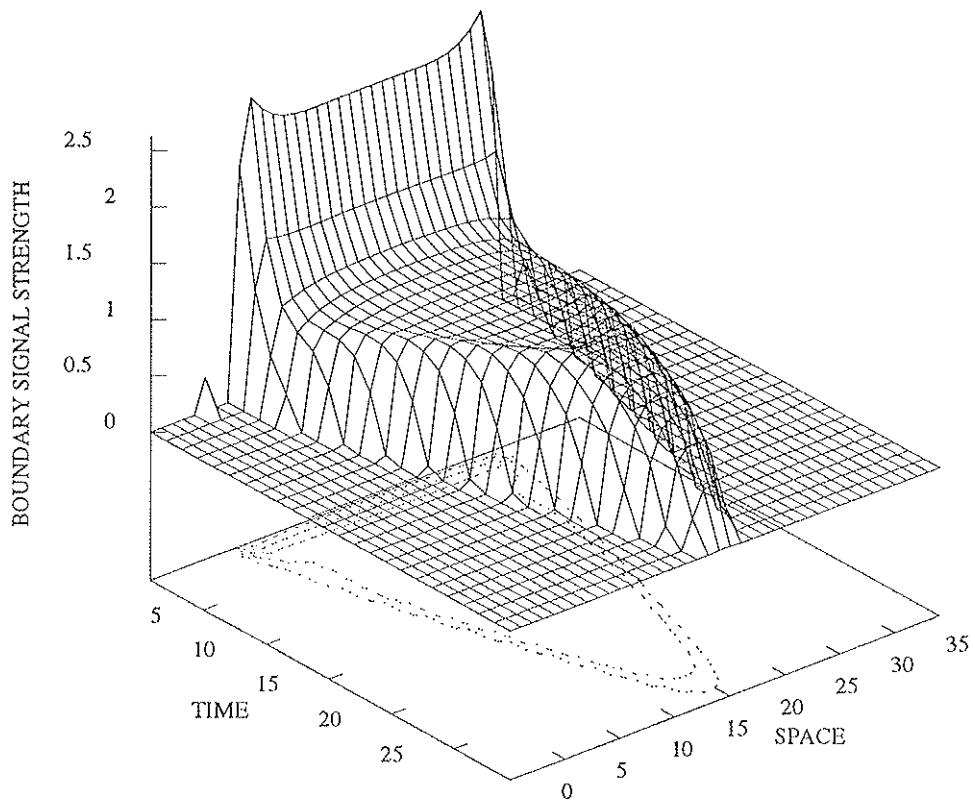


Figure 8:



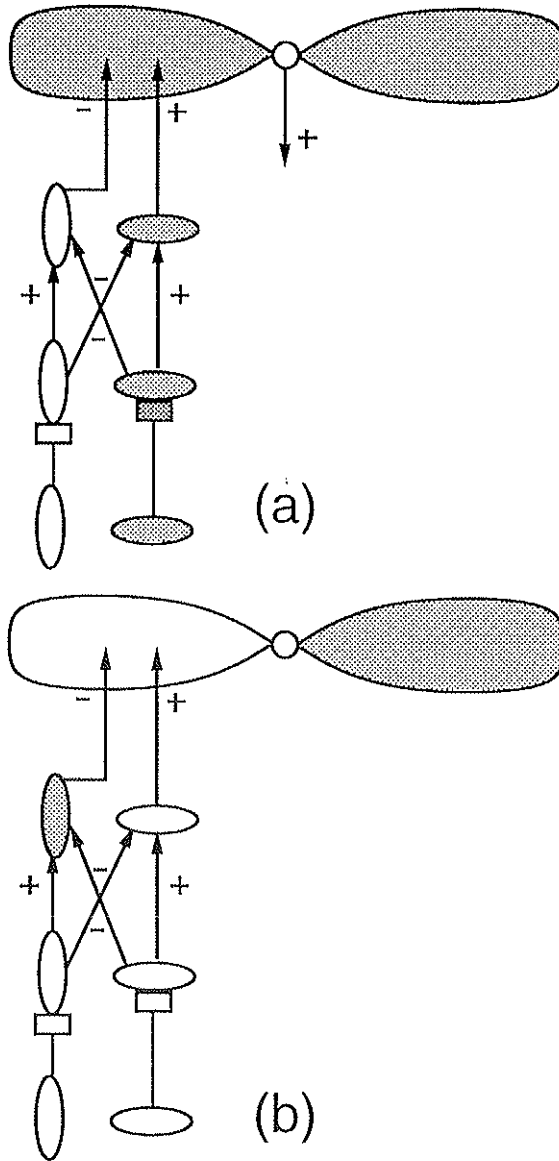
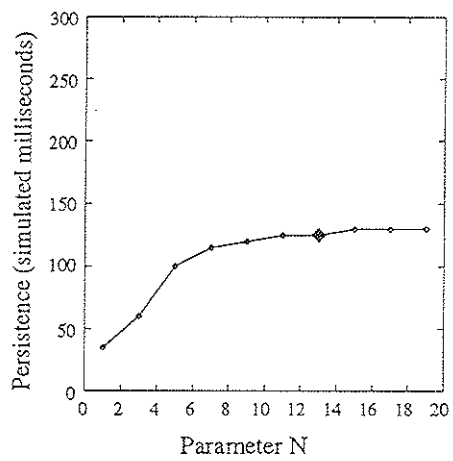
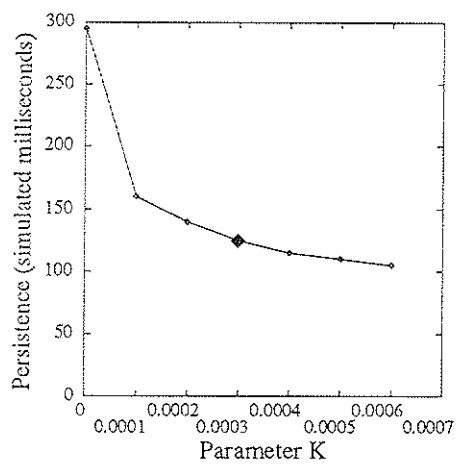


Figure 10:

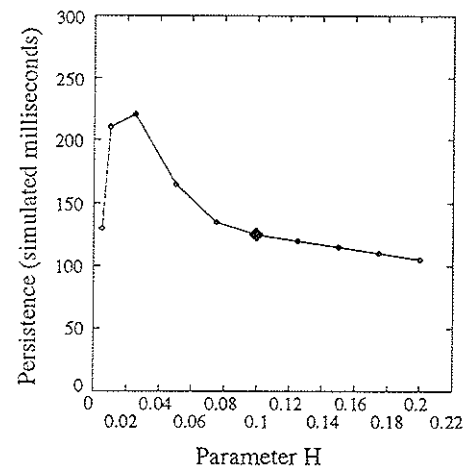
Figure 11:



(a)



(b)



(c)